Advanced Tokamak Research in JT-60U and JT-60SA

Akihiko ISAYAMA for the JT-60 team
Japan Atomic Energy Agency, Naka, Ibaraki 311-0193, Japan

(Received 8 January 2009 / Accepted 8 July 2009)

Results of experiment in JT-60U and design study in JT-60SA (Super Advanced) are described focusing on the development of advanced tokamak. In JT-60U, a high-integrated performance plasma with the normalized beta β_N = 2.6, confinement enhancement factor $H_{H98(y,2)}$ = 1.0-1.1 and bootstrap current fraction f_{BS} = 0.4 has been sustained for 25 s (14 times current diffusion time (τ_R)). Neoclassical tearing mode (NTM) with the poloidal mode number m = 2 and the toroidal mode number n = 1 has been stabilized with modulated electron cyclotron current drive (ECCD) in synchronization with the mode frequency (~5 kHz). A high-beta plasma exceeding the ideal MHD limit without conducting wall has been sustained for 5 s (~3τ_R) by suppressing resistive wall mode (RWM). In addition, two new instabilities in the high-beta regime, *Energetic particle driven Wall Mode* (EWM) and *RWM precursor*, have been observed. In JT-60SA, exploration of full non-inductive steady-state operation with current drive by neutral beams and electron cyclotron waves is planned. In addition, NTM control with ECCD and RWM suppression with external coils are planned.

© *2010 The Japan Society of Plasma Science and Nuclear Fusion Research*

Keywords: advanced tokamak, ITER, hybrid scenario, NTM, RWM, JT-60U, JT-60SA

DOI: 10.1585/pfr.5.S1003

1. Introduction

Steady-state sustainment of high integrated performance is essential for a fusion reactor, where simultaneous achievement of high values of the normalized beta (β_N), confinement enhancement factor ($H_{H98(y,2)}$), non-inductive current drive fraction (f_{NI}) and so on is required. For example, in one of the advanced scenarios in ITER, so called the Hybrid Scenario, β_N = 2-2.5, $H_{H98(y,2)}$ = 1-1.2 and f_{NI} = 0.5 are assumed to obtain the fusion gain Q~5 with the discharge duration of longer than 1000 s [1].

To develop the scenario of the advanced tokamak operation and clarify physics issues and their solution, advanced tokamak research has been extensively performed in JT-60U by fully utilizing its capability. In JT-60U, two major scenarios have been developed for the advanced tokamak research [2]: high-β_p H-mode scenario and reversed shear scenario. Sustainment of high-performance plasmas for longer than current diffusion time has been achieved in both scenarios. This paper focuses only on the advanced tokamak research with the high-β_p H-mode.

In obtaining a stationary high-beta plasma, one of the magnetohydrodynamic (MHD) instabilities to be suppressed or controlled is a neoclassical tearing mode (NTM). The NTM is destabilized by bootstrap current in a plasma with positive magnetic shear and degrades the plasma performance. Among possible mode numbers, NTMs with m/n = 3/2 and 2/1 should be controlled since confinement degradation by them is large. Here, m and n are the poloidal and toroidal mode numbers, respectively.

In JT-60U, two scenarios for NTM suppression have been developed. One is the avoidance of NTM onset through the optimization of pressure and current profiles. To be more specifically, the location of steep pressure gradient, which is typically located at 0.3-0.7 in the averaged minor radius, is adjusted so that it is far from the mode rational surfaces. This scenario is advantageous in that NTMs can be suppressed without additional heating/current drive systems other than those for obtaining the high-performance plasma. In JT-60U, systems for plasma control, heating/current drive and diagnostics were upgraded to obtain a long-duration plasma with auxiliary heating using neutral beams (NBs) and electron cyclotron (EC) waves up to 30 s in 2003 [3, 4]. After the installation of ferritic steel tiles in 2005, a higher-confinement plasma was obtained through the reduction of fast ions [5, 6]. In 2007, pulse width of 3 units of the perpendicular NBs was extended to 30 s, which enabled central plasma heating for longer time.

The other scenario for NTM suppression is active stabilization using electron cyclotron current drive (ECCD). In JT-60U, NTM stabilization has been performed since the installation of the first 110 GHz gyrotron in 1999 [7], and stabilization by real-time mirror steering [8], preemptive stabilization [9] and simulation with the TOPICS code [10–12] have been performed.

In a higher beta regime above the ideal beta limit without conducting wall ('no-wall limit'), a resistive wall mode (RWM) appears and terminates the discharge. RWM had been observed in reversed shear discharges before the installation of the ferritic steel tiles [13]. After the installation of the ferritic steel tiles, RWM study in a positive-

author's e-mail: isayama.akihiko@jaea.go.jp

© 2010 The Japan Society of Plasma Science and Nuclear Fusion Research

shear plasma, which requires higher NB power to reach the no-wall limit, became possible. Detailed scan of toroidal velocity utilizing the capability of various NB injection pattern in JT-60U, the minimum required toroidal rotation velocity was found to be 0.3% of the Alfvén velocity [14].

The operation of JT-60U was concluded with great success in August 2008. A superconducting tokamak, JT-60SA (Super Advanced), is being constructed to take over and drive forward the advanced tokamak research as a combined program of (a) the ITER Satellite Tokamak Program of Japan and EU and (b) the Japanese National Program.

This paper describes results from JT-60U experiments and JT-60SA design study with emphasis on advanced tokamak research. After this introduction, long-duration sustainment of a high-beta plasma through NTM avoidance is described in Sec. 2. Active stabilization of an m/n = 2/1 NTM with modulated ECCD is described in Sec. 3. Suppression of RWM by rotation control and newly observed instabilities are described in Sec. 3. Specifications and research area in JT-60SA is described in Sec. 4. Finally, summary is described in Sec. 5.

2. Long-duration Sustainment of High Integrated Performance Plasma

In JT-60U, the maximum pulse duration of 3 units of NBs was extended to 30 s in 2007, which enabled central heating for longer time. By fully utilizing the capability, long-pulse high-beta experiment with longer duration and higher performance has been performed [15]. Typical discharge of a long-duration high-beta discharge is shown in Fig. 1. Plasma parameters in this discharge are as follows: the plasma current I_p = 0.9 MA, the toroidal field B_t = 1.54 T, the major radius R = 3.36 m, the minor radius a = 0.88 m, the plasma volume V_p = 67 m^3, safety factor at 95% flux surface q_{95} = 3.2. From t = 2.5 s neutral beam was injected stepwise to avoid onset of NTMs. The central value of safety factor q was nearly unity, and large sawtooth oscillation was not observed. The value of the normalized beta, $\beta_N \equiv \beta_t/(I_p/aB_t)$, reached 2.6 by about 10 MW NB injection, and was sustained by feedback control. It can be seen that the injection power is almost the same, and H-mode with edge localized mode (ELM) is sustained stationarily. From t~20 s, D_α intensity and electron density gradually increased, and NB injection power slightly increased, showing confinement degradation. Frequency spectrum of magnetic perturbations (Fig. 1 (c)) shows that no large instability such as NTMs is observed throughout the discharge (See Figs. 4 (c) and 6 (d), where NTM and RWM appear, respectively, for comparison). Although infrequent sawtooth oscillations are observed at ~2 kHz, global confinement degradation is not visible. Profiles of ion and electron temperatures and safety factor at t =27 s are shown in Fig. 2. While the the temperature gradually decreased as the electron density increased, peaked ion and electron temperature profiles were maintained until the end of the high-beta phase. In addition, internal and edge transport barriers were also maintained. It can be seen that the q = 1.5 and 2 surfaces are located at the peripheral region with small temperature gradient, which is effective in avoiding NTM onset.

The value of confinement enhancement factor against the H-mode scaling, $H_{H98(y,2)}$, is 1.0-1.1, and the fraction of bootstrap current to the total plasma current, f_{BS}, is 0.43-0.46 from ACCOME code calculation. These parameters satisfy the requirement for the ITER Hybrid Scenario [1]. Current diffusion time, τ_R, is 1.8 s. Here, $\tau_R \equiv \mu_0 \langle\sigma\rangle a^2/12$, μ_0 is permeability and $\langle\sigma\rangle$ is volume-averaged neoclassical conductivity [16]. Thus, the sustained period in Fig. 1 corresponds to about $14\tau_R$. Actually, safety factor profile

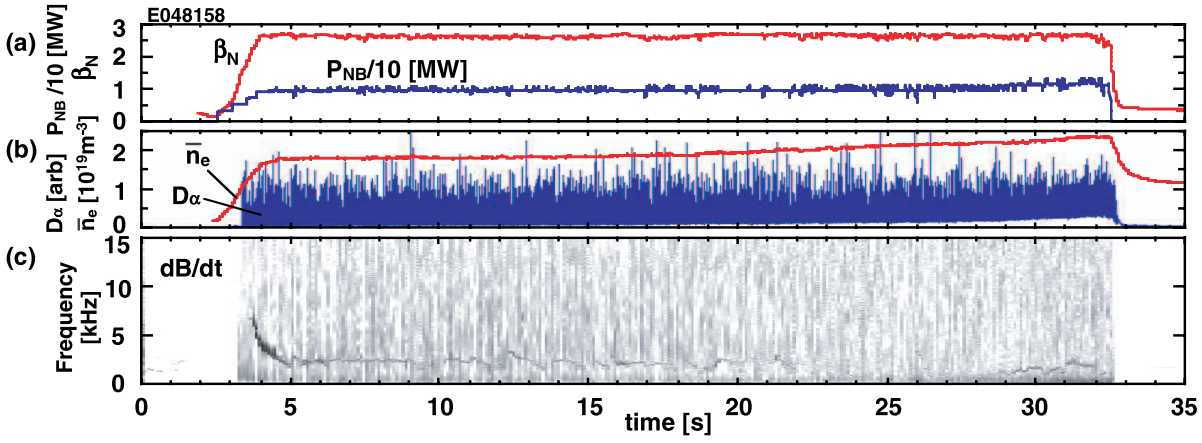

Fig. 1 Typical discharge of a long-pulse high-beta plasma. (a) Normalized beta and NB injection power, (b) line-averaged electron density and D_α intensity, (c) frequency spectrum of magnetic perturbations. The maximum pulse width of the NBs is 30 s, and the duration of the high-beta phase is close to this limit.

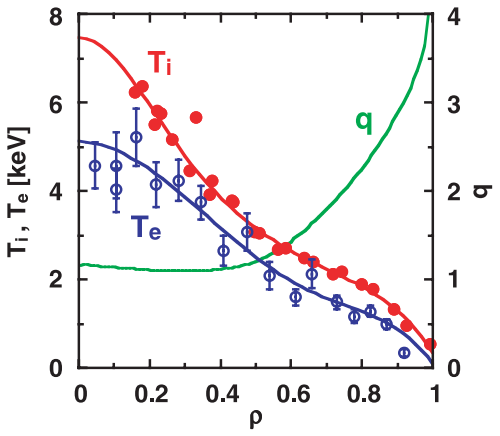

Fig. 2 Profiles of ion and electron temperatures and safety factor at t = 27 s.

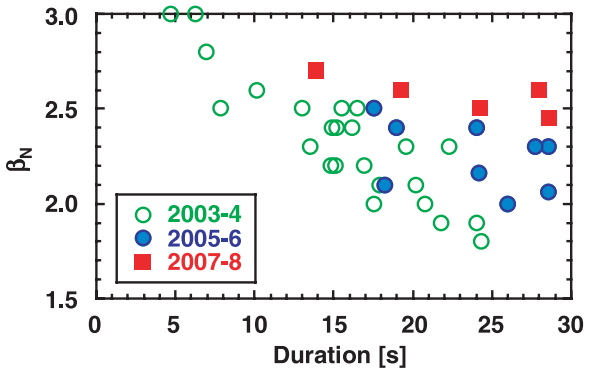

Fig. 3 Progress in the duration of a high beta plasma. Open circles, closed circles and closed squares correspond to the result in 2003-4, 2005-6 and 2007-8, respectively.

measured with motional Stark effect diagnostic is fully relaxed and flat q-profile with $q(0)$~1 is sustained stationarily.

Progress in long-duration sustainment of high-beta plasma is shown in Fig. 3. Before 2003, confinement was not high ($H_{H98(y,2)}$~0.8-0.9) although pulse duration was significantly increased from 10 to 30 s, and β_N = 2.3 was sustained for 22.3 s [3, 4]. Insertion of ferritic steel tiles contributed to extending the pulse duration as well as enhancing the confinement by reducing loss power and thus increasing available power in the later phase of discharges. Extension of the pulse width of the 3 perpendicular NBs in 2007 made it possible to further extend the duration of high-beta plasma, and as shown in Fig. 3, β_N = 2.6 was sustained for 25 s, and β_N = 2.3 was sustained for 28.6 s. Note that in addition to the extension of the NB pulse width, confinement improvement due to the central heating also contributed to extending the operational regime because reduction of NB power to sustain a given beta value contributes to extending the pulse width under a fixed injection energy. Since the maximum pulse duration in the present JT-60U system is 30 s, the sustained period is nearly equal to the maximum pulse width of the NBs.

3. Active Stabilization of Neoclassical Tearing Mode by Localized Electron Cyclotron Current Drive

In JT-60U, modulation frequency of the output power of gyrotrons has been increased year by year through continuous modification and conditioning. In 2008, modulation at about 7 kHz was successfully achieved [17, 18]. For NTM stabilization with modulated ECCD, EC wave is needed to be synchronized with the rotation of the NTM. In JT-60U, magnetic probe was used to generate a trigger signal for the modulation of gyrotron power. In addition, control system for the gyrotrons has been upgraded so that modulation frequency can be changed automatically to follow the change in the mode frequency by monitoring the magnetic probe signal in real time [18]. By using this system, phase difference between the magnetic perturbations and the modulated EC wave power can be fixed even if the NTM frequency changes in time during a discharge [18]. In 2008, stabilization of an m/n = 2/1 NTM with modulated ECCD was performed [19].

Typical discharge waveforms and plasma cross section in an NTM stabilization experiment are shown in Fig. 4, where typical plasma parameters are as follows: I_p = 1.5 MA, B_t = 3.7 T, R = 3.18 m, a = 0.80 m, q_{95} = 4.1. In this series of discharges, NBs of about 25 MW was injected to destabilize a 2/1 NTM, and β_N increased to about 2. Ion temperature, electron temperature and electron density at the center are about 20 keV, 10 keV and 3×10^{19} m^{-3}, respectively. An m/n = 2/1 NTM appeared at t~5.7 s, and the value of β_N decreased to about 1.2. At t = 6.7-7 s, NB power was decreased, and the direction of the tangential NBs was changed from balanced injection to counter injection to raise the mode frequency. The 2/1 NTM started to rotate in the counter direction at t = 7.5 s, and the mode frequency reached about 4-5 kHz as shown in Fig. 4 (c). The mode frequency is almost linearly proportional to the toroidal rotation velocity at the mode location. Electron cyclotron wave with the frequency of 110 GHz was injected at t = 9.5 s from the low-field side as shown in Fig. 4 (d). The 2/1 mode is located at ρ~0.6, where ρ is volume averaged normalized minor radius. According to calculation with ACCOME and EC-Hamamatsu codes, the total EC-driven current is 3 kA, and the peak EC-driven current density corresponds to ~20% of bootstrap current density at the q = 2 surface.

Temporal evolution of magnetic perturbation amplitude is shown in Fig. 5 (a), where phase difference between magnetic probe signal and gyrotron power P_{gyr} is 0°, 90° and 180°. For the 0° case, the mode amplitude decreases during the ECCD. For the 90° case, no clear effect of ECCD is seen, and for the 180° case, increase of mode amplitude, that is, NTM destabilization is observed. Detailed scan of the phase difference shows that O-point ECCD corresponds to the case when the phase difference is about −10°. Thus, the 0° case and the 180° case nearly corre-

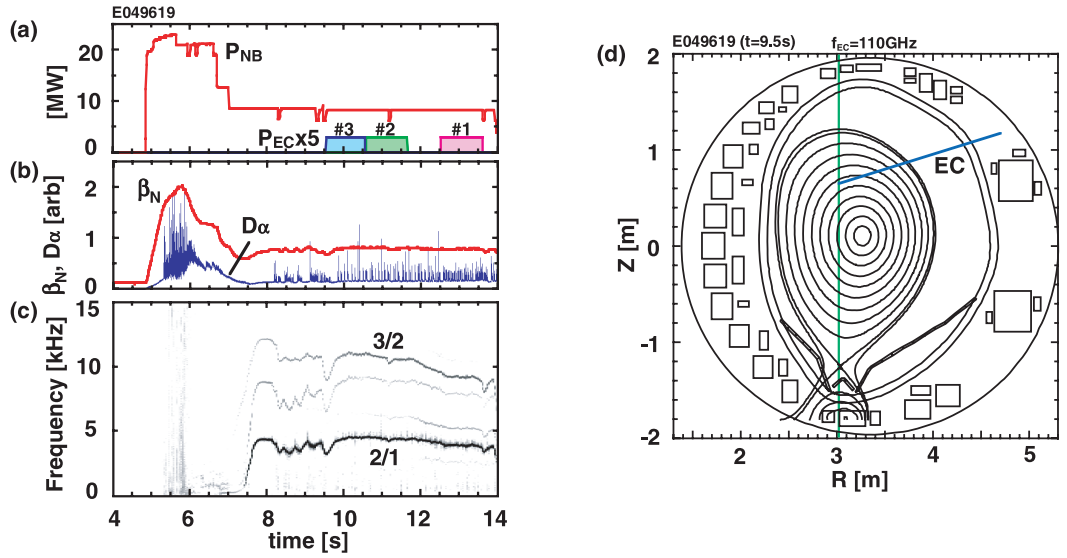

Fig. 4 Typical discharge of stabilization of an $m/n = 2/1$ NTM with ECCD. (a) Injection power of NB and EC wave, (b) the normalized beta and D_α intensity, (c) frequency spectrum of magnetic perturbations, (d) plasma cross section. In Fig. 4 (d), contour is drawn every 0.1 in the volume-averaged normalized minor radius.

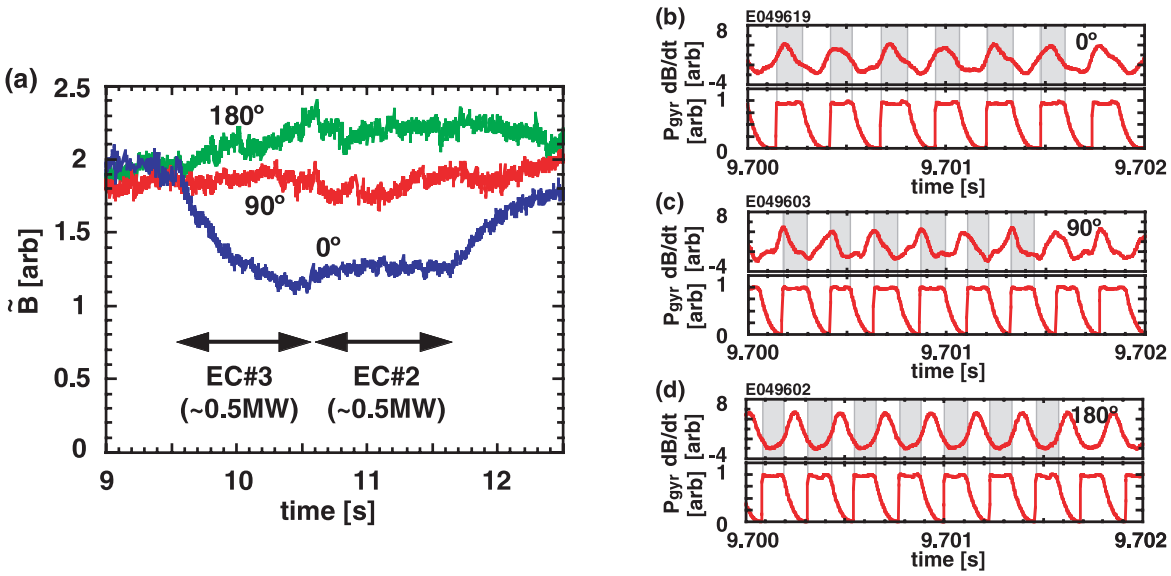

Fig. 5 (a) Temporal evolution of magnetic perturbation amplitude for different phase difference between the magnetic probe signal and EC wave power. Waveforms of magnetic perturbation and gyrotron power for the phase difference of (b) 0°, (c) 90° and (d) 180°.

spond to O-point ECCD and X-point ECCD, respectively. From this figure, it can be seen that phase difference should be properly controlled to stabilize an NTM efficiently. Expanded figure of magnetic probe signal and gyrotron power for each case is shown in Figs. 5 (b)-(d). As shown in these figures, the phase difference is successfully scanned by using the newly developed system. It was also found that the stabilization effect defined by the initial decay time of the magnetic perturbation amplitude increases with deviating from the optimum phase difference: the decay time is doubled when the deviation becomes ±50°.

It was considered that modulated ECCD is more effective in stabilizing an NTM than unmodulated ECCD. However, experimental verification for an $m/n = 2/1$ NTM had not been done yet. In JT-60U, it was found that the initial decay time for modulated ECCD is less than half of that for unmodulated ECCD with almost the same (peak) EC wave power. This shows that required EC wave power can be reduced significantly by modulating the EC wave although experimental verification is remained as future work. According to the modified Rutherford equation, which describes the NTM evolution, the ECCD efficiency is equivalent to the inverse of the initial decay time, suggesting that the required EC wave power for NTM stabilization can be

reduces as small as this value. Detailed evaluation of the required EC wave power using the TOPICS-IB code is also remained as future work.

4. Long Duration Sustainment of High-beta Plasmas Above No-wall Limit through Resistive wall Mode Suppression

In the 2008 campaign, experiments on high-beta plasmas above the no-wall limit are focused on the extension of the duration [20]. Typical discharge of a high-beta discharge is shown in Fig. 6, where plasma parameters are as follows: I_p = 0.9 MA, B_t = 1.44 T, R = 3.43 m, a = 0.91 m, q_{95} = 3.2. As shown in Fig. 6 (a), the plasma volume is relatively large to enhance the wall stabilization effect, but not so large as to increase metal impurity from the wall. In this discharge, beta value was first increased by positive-ion-based NBs (P-NBs) alone, and then some of the perpendicular NBs were turned off to replace with negative-ion-based NBs (N-NBs). (Note that in JT-60U there are 11 units of P-NBs, and 7 of them are in the perpendicular direction, 2 of them are in the tangential and co-direction and 2 of them are in the tangential and counter-direction. Note also that there are 2 units of N-NBs, and they are in the tangential and co-direction.) The change of the injection pattern is effective in avoiding the instabilities which trigger RWMs (described later) by increasing in the plasma rotation velocity and at the same time reducing trapped particle component of fast ions. The value of the normalized beta was kept at ~3.0 by feedback control on NBs. The no-wall beta limit, $\beta_N^{\text{no-wall}}$, calculated by an ideal MHD stability code MARG2D [21] is ~2.6, which corresponds to $3.0\ell_i$. Here, ℓ_i is the internal inductance. The beta limit with an ideal wall, $\beta_N^{\text{ideal-wall}}$, is calculated to be ~3.2 corresponding to $3.8\ell_i$. The sustained β_N value of 2.9 corresponds to C_β = 0.3. Here, C_β is defined as $C_\beta \equiv (\beta_N - \beta_N^{\text{no-wall}})/(\beta_N^{\text{ideal-wall}} - \beta_N^{\text{no-wall}})$, and it indicates how close to the ideal wall limit the beta value is. In this discharge, the no-wall beta limit gradually increases in time due to current penetration and β_N becomes smaller than $3\ell_i$ at t = 11.2 s. The duration of high beta above the no-wall limit is about 5 s, which corresponds to 3 times the current diffusion time. Progress in the sustained duration of high-beta plasmas above the no-wall limit is shown in Fig. 7. Note that all of the data points are the ones with $\beta_N > \beta_N^{\text{no-wall}}$. In the 2005-6 campaign, the duration was limited to less than 1.6 s due to the onset of NTMs and RWMs. The duration was also limited by reaching the beta value below the no-wall limit due to current penetration (i.e. increasing in ℓ_i). In the 2007-8 campaign, by optimizing the discharge scenario, NTM and RWM were successfully avoided, and current penetration was delayed, which resulted in extending the operational regime.

In this series of discharges, two kinds of instabilities appeared and limited the discharge duration through the onset of RWM: one is a fishbone-like instability termed *Energetic particle driven Wall Mode* (EWM), and the other is a slowly glowing mode termed *RWM precursor*. Both instabilities are observed only at $\beta_N > \beta_N^{\text{no-wall}}$, and one of them or both of them appeared in many of the high-beta discharges. Figure 8 shows an example where both EWM and RWM precursor are observed before an RWM. It is found that the EWM is triggered by an ELM or an EWM and has the following characteristics: (a) the growth and decay

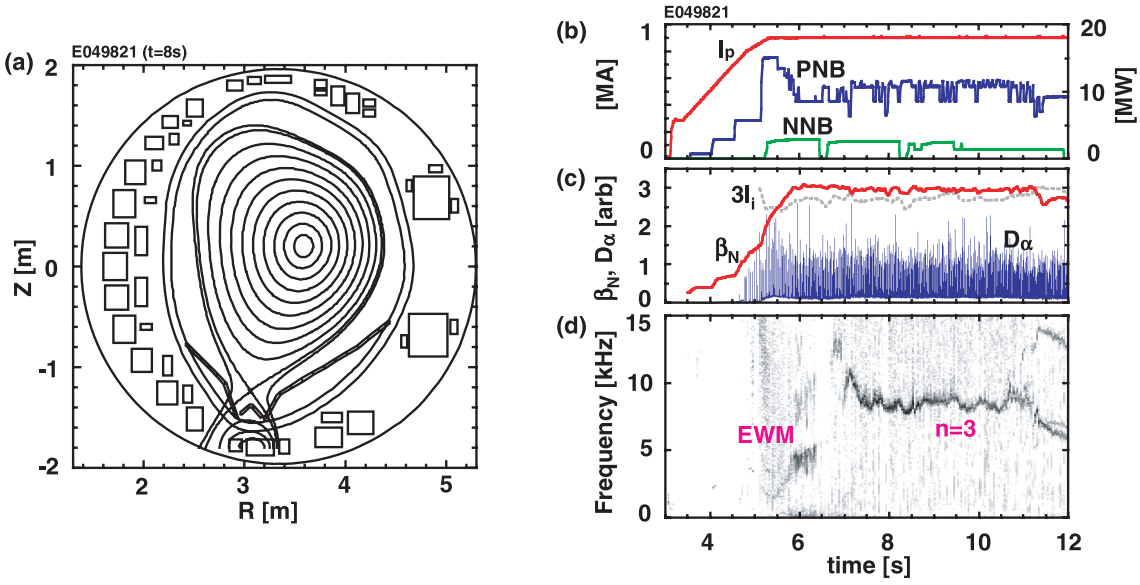

Fig. 6 Typical discharge of sustainment of a high-beta plasma above the no-wall limit. (a) Plasma cross section, (b) plasma current and injection power of NB, (c) normalized beta and D_α intensity and (d) frequency spectrum of magnetic perturbations.

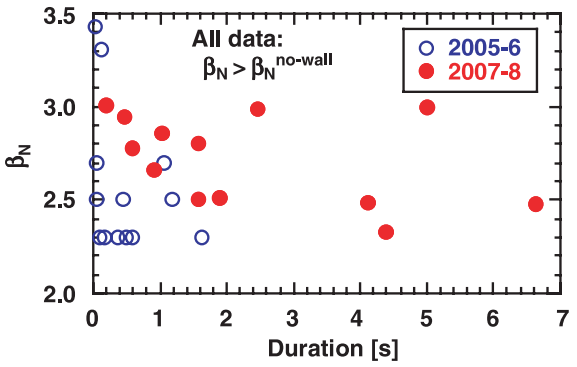

Fig. 7 Sustained value of the normalized beta versus duration. All data reach a beta value above the no-wall limit. Open circles and closed circles correspond to the data in 2005-6 and 2007-8, respectively.

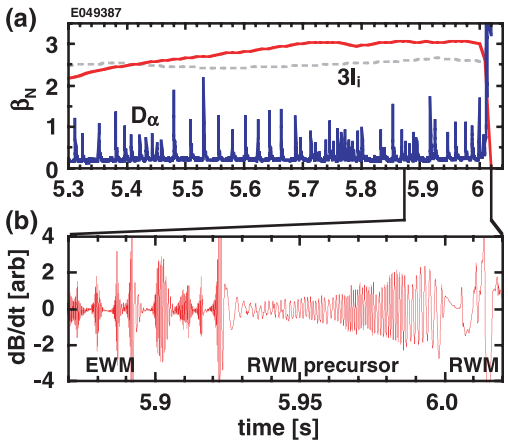

Fig. 8 Example of EWM and RWM precursor. (a) β_N and D_α intensity and (b) expanded figure of magnetic perturbations.

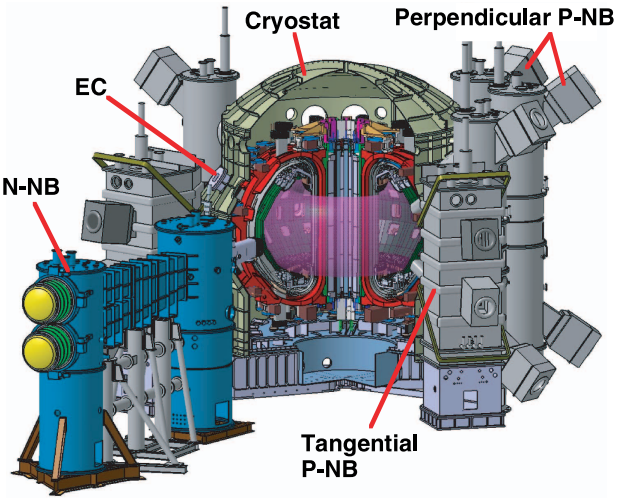

Fig. 9 Birds-eye view of JT-60SA. P-NB, N-NB and EC wave systems are equipped for auxiliary heating and current drive.

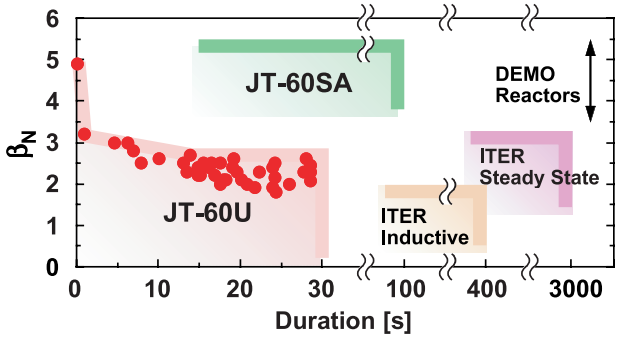

Fig. 10 Operational regime in JT-60SA. Also shown are the operational regimes in JT-60U, ITER Inductive scenario and ITER Steady State Scenario and DEMO.

time are a few milliseconds, which is comparable to the resistive wall time τ_w, (b) $n = 1$ and $m = 3$-4, (c) no phase inversion in electron temperature measured with electron cyclotron emission diagnostics, that is, no island structure, (d) much larger amplitude at the low-field side than at the high-field side, (e) frequency chirping and (f) mode amplitude correlating with the power of perpendicular NBs. The EWM is different from the so-called fishbone instability in that the EWM is observed even when the central safety factor is above unity. The RWM precursor has the following characteristics: (a) the growth time is 10-50 ms ($\gg \tau_w$), (b) $n = 1$ and $m = 2$-3, (c) no island structure, (d) a kink-ballooning-like mode structure and (e) it decreases V_t and/or dV_t/dr. In this series of experiments, it was found that the EWM appears and triggers RWM even when rotation velocity and its shear are enough high for RWM stability. In addition, the RWM precursor decreases the rotation velocity and its shear and triggers RWM. This shows that control of energetic particles and rotation velocity/shear is important for RWM stabilization.

5. Target of AT Research in JT-60SA

The JT-60SA device, which has 18 toroidal coils and 6 poloidal coils with superconducting magnets, will be installed in the present JT-60 torus hall [22, 23]. A birds-eye view of JT-60SA is shown in Fig. 9. The mission of JT-60SA is early realization of fusion energy by supporting exploitation of ITER and performing research toward DEMO. The maximum plasma current is 5.5 MA with a low aspect ratio (~2.5) plasma, and ~3 MA for an ITER-shaped plasma. Inductive operation with a flat top duration up to 100 s will be possible within the total available flux swing. JT-60SA is characterized by its high value of the shape factor $S = (I_p/aB_t)q_{95} \propto A^{-1}\{1 + \kappa^2(1 + 2\delta^2)\}$. Here, $A = R/a$ is the aspect ratio, κ is the plasma elongation and δ is the plasma triangularity. Since plasma stability at the core and/or edge is improved by increasing A^{-1}, κ and δ, S is considered to be a measure of stability improvement. In addition, by its definition, the toroidal beta ($= S\beta_N/q_{95}$) increases with S if β_N/q_{95} is the same [24]. Since the value of S in JT-60SA is typically 6, and it is much larger than

that in JT-60U (~ 2), higher stability is expected. Target of the operational regime in JT-60SA is shown in Fig. 10. The beta value is higher than the no-wall limit, and the duration is much longer than that in JT-60U. As auxiliary heating and current drive tools, P-NB, N-NB and EC wave systems are installed. Since the plasma in such a high-beta regime is vulnerable to NTM and RWM, control of these instability is an important issue in JT-60SA. For RWM control, in-vessel coils are to be installed in addition to passive conducting wall. For NTM control, the 110 GHz EC wave system will be reused with improvements in the pulse width and power. Other components for the JT-60U facility, such as NB and diagnostic system, will be reused. Since the heating/current drive system is needed to be upgraded for the JT-60SA operation, R&D activities are being done in parallel with the construction.

6. Summary

Significant progress has been made in JT-60U advanced tokamak research until the very end of its experimental campaign in August 2008. A high-integrated performance plasma with β_N~2.6, $H_{H98(y,2)}$ = 1.0-1.1, f_{BS}~0.4, which satisfies the requirement of the ITER Hybrid Scenario, has been stationary sustained for 25 s ($14\tau_R$). Stabilization of an m/n = 2/1 NTM with modulated ECCD has been successfully performed by modulating EC wave at ~5 kHz in synchronization with mode frequency. The superiority of modulated ECCD to unmodulated ECCD by a factor more than 2 has been shown experimentally. A high-beta plasma above the no-wall limit has been sustained for ~5 s (~$3\tau_R$). Two new instabilities which appear only at $\beta_N > \beta_N^{\text{no-wall}}$, energetic particle driven wall mode (EWM) and RWM precursor, have been observed. Design activity for JT-60SA is undergoing. Physics assessment is also being done for advanced tokamak research.

[1] M. Shimada, D.J. Campbell, V. Mukhovatov *et al.*, Nucl. Fusion **47**, S1 (2007).

[2] Y. Kamada, T. Fujita, S. Ishida *et al.*, Fusion Sci. Technol. **42**, 185 (2002).

[3] S. Ide and the JT-60 Team, Nucl. Fusion **45**, S48 (2005).

[4] A. Isayama and the JT-60 Team, Phys. Plasmas **12**, 056117 (2005).

[5] H. Takenaga and the JT-60 Team, Nucl. Fusion **47**, S563 (2007).

[6] N. Oyama, A. Isayama, T. Suzuki *et al.*, Nucl. Fusion **47**, 689 (2007).

[7] Y. Ikeda, A. Kasugai, S. Moriyama *et al.*, Fusion Sci. Technol. **42**, 435 (2002).

[8] A. Isayama, Y. Kamada, N. Hayashi *et al.*, Nucl. Fusion **43**, 1272 (2003).

[9] K. Nagasaki, A. Isayama, S. Ide *et al.*, Nucl. Fusion **43**, L7 (2003).

[10] N. Hayashi, A. Isayama, K. Nagasaki *et al.*, J. Plasma Fusion Res. **80**, 605 (2004).

[11] K. Nagasaki, A. Isayama, N. Hayashi *et al.*, Nucl. Fusion **45**, 1608 (2005).

[12] A. Isayama, N. Oyama, H. Urano *et al.*, Nucl. Fusion **47**, 773 (2007).

[13] S. Takeji, S. Tokuda, T. Fujita *et al.*, Nucl. Fusion **42**, 5 (2002).

[14] M. Takechi, G. Matsunaga, N. Aiba *et al.*, Phys. Rev. Lett. **98**, 055002 (2007).

[15] N. Oyama, A. Isayama, G. Matsunaga *et al.*, Nucl. Fusion **49**, 065026 (2009).

[16] D.R. Mikkelsen, Phys. Fluids B **1**, 333 (1989).

[17] S. Moriyama, T. Kobayashi, A. Isayama *et al.*, Nucl. Fusion **49**, 085001 (2009).

[18] T. Kobayashi, M. Terakado, F. Sato *et al.*, Plasma Fusion Res. **4**, 037 (2009).

[19] A. Isayama, G. Matsunaga, T. Kobayashi *et al.*, Nucl. Fusion **49**, 055006 (2009).

[20] G. Matsunaga, Y. Sakamoto, N. Aiba *et al.*, *Fusion Energy 2008* (Proc. 22nd IAEA Fusion Energy Conf., Geneva (IAEA, Vienna)) IAEA-CN-165/EX/5-2 (2008); G. Matsunaga, N. Aiba, K. Shinohara *et al.*, Phys. Rev. Lett. **103**, 045001 (2009).

[21] S. Tokuda and T. Watanabe, Nucl. Fusion **6**, 3012 (1999).

[22] M. Kikuchi, *Fusion Energy 2006* (Proc. 21st IAEA Fusion Energy Conf., Chengdu (IAEA, Vienna)) IAEA-CN-149/FT/2-5 (2006).

[23] M. Matsukawa, M. Kikuchi, T. Fujii *et al.*, Fusion Eng. Des. **83**, 795 (2008).

[24] E.J. Strait, Phys. Plasmas **1**, 1415 (1994).